Solid State Technology
Volume: 63 Issue: 2
Publication Year: 2020

Modification of Nickel-phosphor Electroless Coatings by adding particles of Zirconia

Nabaa S. Radhi [1], Marwa Marza [1] & Zainab S. Al-Khafaji [2*]
[1] University of Babylon /College of Materials Engineering, Babil/Iraq.
Email: dr.nabbaa@gmail.com, marwamarzas@gmail.com
[2] Al-Furat Al-Awsat Distribution Foundation, Ministry of Oil, Babylon, Iraq;
[2] Department of Civil Engineering, Al-Mustaqbal University College, Babylon, 9CW3+4G Hilla, Iraq
https://orcid.org/0000-0002-5450-7312
*Corresponding Author** zainabcivil90@gmail.com & ZainabAl-khafaji@mustaqbal-college.edu.iq

Abstract- Researchers have devoted much time to metal deposition processes via the deposition of electroless nickel, alloy & composite coatings on different surfaces; most recent applications have been made possible due to different excellent characteristics of these coatings. These coatings have recently shown exciting properties in terms of wear & corrosion resistance, leading to several novel innovations for macro-level applications. In this work, the concept of composite coating via co-deposition coating was introduced. The improvement in the properties of the Ni-P alloy coatings was evaluated by introducing Zr particles into the electroless deposited solution. The stainless steel (SS) samples were first coated using electroless with Ni-P and Zr microparticles (size = 30- 70 µm) at different concentrations of 0, 10, & 20 g/L. The samples were subjected to SEM and AFM analysis after being impeded in NaCl solution (3.5%) for corrosion behaviour study before the wear resistance and microhardness tests.

The results of this study revealed a significant decrease in the corrosion currents due to the presence of inert particles. The corrosion and wear tests revealed similar improvements as well.

Keywords: *Composite coatings; Electroless nickel-phosphorus; stainless steel, Zirconia, microhardness and wear resistance properties*.

1.1 Introduction:

Electroplating is commonly considered as the traditional electrolytic plating process. It is achieved when metal ions are first reduced to their respective metallic states before deposition at the cathode under the influence of an external electrical source (A Brenner & Riddell, 1946). Electroless plating can be likened to a chemical reduction process in many aspects even though they differ significantly. It involves the catalytic reduction of metallic ions in a reducing agent-containing aqueous solution, followed by the subsequent deposition of the metal in the absence of any external energy source (Abner Brenner, 1946; none, 2009; N.S. Radhi & Al-Khafaji, 2018).

The chemical reduction of nickel results in the formation of the electroless nickel deposit; however, this process is dependent on the type of reducing agent used. For instance, nickel-phosphorus coatings are produced when hypophosphite is used as the reducing agent (Al-khafaji et al., 2018; Domenech et al., 2003). Hence, the reaction must be controlled to ensure the occurrence of the reduction only on the substrate without affecting the equipment used during the process. This mechanism can be controlled by adding some additives to the reaction baths; such additives may include complexing agents, stabilizers, and pH regulators. Stabilizers are commonly used additives when working under stable and adequate conditions for long periods (Al-Zubaidy et al., 2019; Mallory & Hajdu, 1990). Composite materials co-deposition using electroless coatings

is referred to as electroless composite coatings. The co-deposition of fine particulate matters can result in wear-resistant composites; studies have reported the co-deposition of hard particles like silicon carbide, diamond, and solid lubricants like polytetrafluoroethylene (PTFE) particles (Al-Mimar et al., 2018; Balaraju et al., 2003; Nabaa S Radhi, 2015; Yaseen et al., 2019). However, early attempts at electroless composite coatings failed and often resulted in bath decomposition due to the increase in the surface area loading of the bath upon the dispersion of the fine particles; this increase in surface area loading (about 700-800 times of the normal bath) cause the bath to exhibit a high level of instability. However, it has been possible to prepare electroless nickel composite coating using the with the appropriate stabilizers. Electroless coating permits accurate surfaces regeneration and prevents subsequent mechanical finishing (Agarwala & Agarwala, 2003; Sahoo & Das, 2011).

The development of electroless coatings relies on the impact and settling of particles on the workpiece surface, followed by the deposition of Ni-P matrix, which will surround these particles. No form of molecular bonding exists between the introduced fine particles and the metal matrix. Guglielmi has proposed a mathematical model for composite coatings electro-deposition. The outcome of the experiments agreed with the proposed mechanism by (Guglielmi, 1972). Furthermore, Grosjean et al. reported an experimental set-up for electroless Ni-SiC composite coatings production (Grosjean et al., 2000); the study relied on the agitation induced by the circulating fluid. The bath circulation (top to bottom) generated a laminar fluid flow on the sample surface; this type of cell provided the agitation, and one of its advantages is that the particles are kept in suspension within the solution.

Another study by Apachitei et al. (Apachitei et al., 1998; Nabaa S. Radhi et al. Nabaa S. Radhi et al., 2018) demonstrated that Al_2O_3 particles (spherical shaped) exhibited better incorporation compared to irregularly shaped ones; the shape of the particle also determines the type of finish of the deposit. Large angular and small rounded particles normally give rough and smooth surfaces, respectively. Many authors have investigated particles such as SiC, CrC, ZrO_2, Al_2O_3, PTFE, and graphite (Dawood et al., 2020; Grosjean et al., 2001; Li, 1997).

Nanosized diamond particles (0.52-2.21 wt.%) have been reported to exhibit a surface change from bright & smooth to foggy & rough appearance with the nodular surface in the electroless Ni-P matrix (Xiang et al., 2001). Another study reported obtaining Ni-P composite coatings via the introduction of SiC & Si_3N_4 to investigate their influence on the coating properties and the co-deposition process. The study noted modifications in the mechanism of growth of the metallic matrix by the nanosized particles compared to the micron-sized ones (Sarret et al., 2006).

In this work, the aim is to study theeffect of the introduced ZrO_2 particles on the structural and mechanical characteristics of the product in comparison to SS 316L substrate.

2. Experimental work

2.1 Electroless Procedures

Table 1 showed the chemical composition of the SS316L sample used in this study. The sample was chemically analyzed using a spectroscopy device for metal materials.

Table (1) Chemical composition of the sample used.

Element	C	Si	Mn	P	Cr	Mo	Ni	Al	Cu	Fe
Percentage%	0.019	0.442	0.854	0.046	16.71	2.09	10.07	0.0012	0.356	Rem

All the samples for the experiments were cylindrical while the finals samples were disc-shaped, of thickness = 3mm, diameter = 12 mm, and surface area = 3.391 cm^2.

The preparation of the surface of the sample was done by:

1. Firstly pulverizing the sample surface with Grit silicon carbide papers of different grades (220, 240, 400, 600, 800, 1000, 1200), followed by surface cleaning with brine and acid; the cleaning process was done in preparation for the electroless process based on the required period per sample.
2. Then the surface was then pretreated for substrate deposition; the substrates were first cleaned with NaOH (10%) for 10–20 min at 60– 80 °C to clean off grease, then, it was rinsed with water and dipped in HCl (5%) for 30 sec for surface activation before rinsing in deionized water before electro-less (Ashtiani et al., 2017).
3. Table 2 presents the chemical composition and operating conditions of the plating baths. The deposition process was carried out in a 150 mL bath that was maintained at 90± 1°C for 80 min. NaOH was used to regulate the pH of the solution to 5. The particles were prevented from sedimentation by using a magnetic stirrer at a rotation rate of 300 rpm.

Table (2) Components of electroless solution, (Ashtiani et al., 2017).

Solution	Chemical composition for 150ml	Condition of Deposition
Ni-P Solution	Nickel sulfate =30 g/l Sodium hypophosphite =25 g/l Sodium citrate =20 g/l Thiourea= 2mg/l ZrO_2=0, 10 and 20 g/l Nano scale , d (30-70) nm	pH = 5 Temp=90± 1 °C. Coating time= 80 min bath stirring rate 300 rpm.

Figure 1 presents the schematic sketch and the actual electroless set-up used in the present study. The temperature of the plating bath was monitored using a thermometer that was inserted into the electroless plating bath. An inert rod or thread was used to immerse the substrate inside the electroless bath after cleaning and activation. The substrates were kept inside the plating bath for a specific period to obtain a coating thickness of ~ 30 μm or more. To ensure the right plating thickness is achieved, the required plating time was maintained based on the plating rate. The as-plated coatings were washed in deionized water and dried in air. The same process as repeated for all the electroless Ni-P and Ni-P-ZrO_2 (10 and 20 g/l) alloy coatings to ensure uniform substrate coatings.

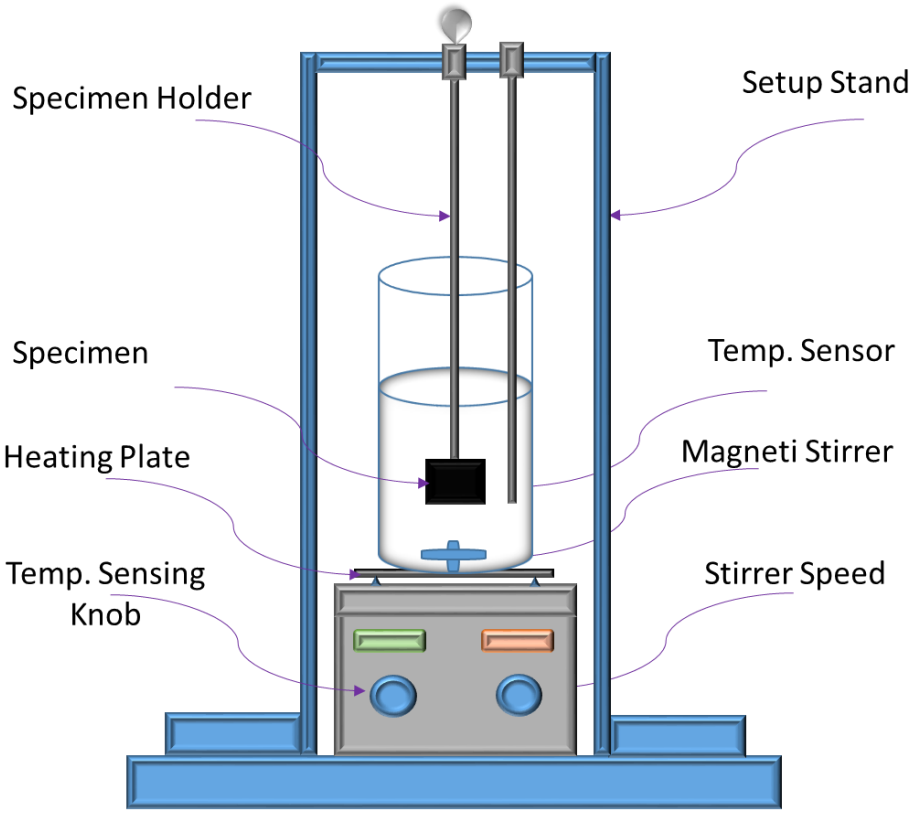

Fig. (1) Electroless coating process apparatus.

2.2 Tests:

For evaluating the performance of the coating layers in this research, the following tests were carried:

2.2.1. Thickness Test

The thickness of the Ni-P, Ni-P-10ZrO_2, & Ni-P-20ZrO_2 layer was measured using a thickness measuring device.

2.2.2. Scanning Electron Microscope (SEM)

Some of the characteristics of the grain boundaries were measured by identifying and measuring the phases, shape, and grain size. And each of these parameters has a specific characteristic. The microstructure of the Ni-P, Ni-P-10ZrO_2 and Ni-P-20ZrO_2 layers was evaluated using contact mode SEM at 2.50 kx magnification

2.2.3 Atomic Force Microscope:

Atomic force microscopy (AFM, contact mode, spm AA3000 Angstrom advanced Inc., USA) was used to observe the morphology (Roughness, depth morphology of film) for Ni-P, Ni-P-10ZrO_2 and Ni-P-20ZrO_2 layers.

2.2.4. Hardness Test

The hardness of the Ni-P, Ni-P-10ZrO_2 and Ni-P-20ZrO_2 layers was measured using TH-717 Digital Micro Vickers Hardness Tester at the condition of 200 N load and 20-sec holding time.

2.2.5 Wear resistance test:

The SS, Ni-P, Ni-P-10ZrO_2, and Ni-P-20ZrO_2 samples were prepared with a diameter of 12 mm and a thickness of 3 mm following ASTM (G99-04) guidelines (Kadhim & Al-Rufaye, 2016). The weight of the samples was determined using a sensitive electric balance model with $\pm$0.0001 accuracy. For studying the dry wear, the pin on disk concept was used on the wear tester device. The samples were set as a pin against a standard rotating steel disk of 850 HV hardness (where: Normal force on the pin (F) = 10 N, Pin diameter (d) = 10 mm, Disk

diameter =30 mm, Wear track radius (R) = 5 mm, Disk rotation speed (ω) = 300 rpm). The lost weight of the specimens was determined by weighted them after 5, 10, 15, and 20) min. Then, weight loss was converted to volume loss according to the following equation:

Volume loss (mm^3) = $weigh\ t\ loss\ (g)/\ density\ (g/mm^3)$ …(1)

Where: weight loss = weight before the test – weight after the test.

3. Results and discussion:

3.1 Thickness Results

The observed weight loss was converted to volume loss using the following relation: The thickness of the coating specimens was 30.7 µm for Ni-P, 34.5 µm for Ni-P-10ZrO_2, and 37.9 µm for Ni-P-20ZrO_2, showing that the deposit rates of the last coating layers were great. The reason for this observation could be the ZrO_2-induced high diffusivity of the specimens as the rate of thickness was found to improve with increases in the particles size and amount of the ZrO_2 layer (Table 3).

Table (3): The Thickness of (Ni-P-) Layer Coating.

Samples	Thickness (µm)
Ni-P	30.7
Ni-P-10ZrO_2	34.5
Ni-P-20ZrO_2	37.9

3.2. Scanning Electron Microscope (SEM)

The SEM micrographs of the samples at different zirconia contents were shown in Figure 3. The figures also showed the influence of the ZrO_2 content on the thickness of the coatings. ZrO_2 particles were deposited in clusters that resemble an aggregated composition on the base metal.

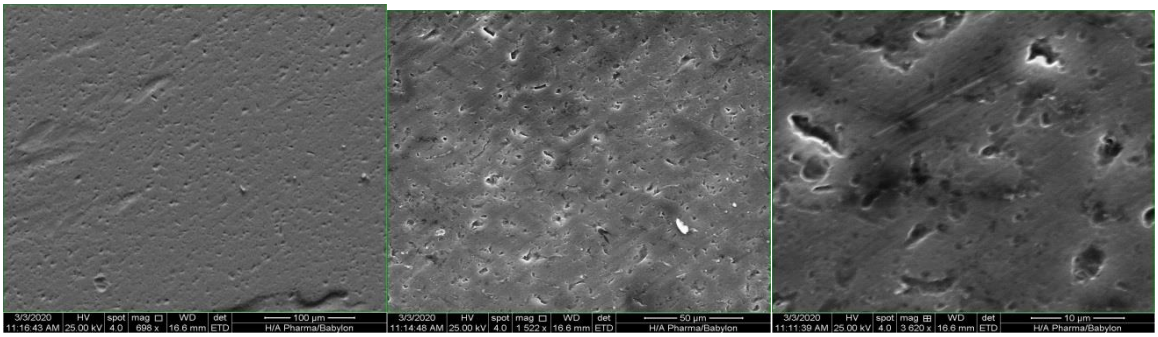

(a) **(b)** **(c)**

(a): Ni-P (b): Ni-P-10ZrO_2, (c): Ni-P-20ZrO_2

Figure (3) SEM topographic morphology for coating layers at (2000x) magnification.

3.3 Atomic Force Microscope (AFM)

The topography of the coating thickness layer for the samples was determined using the atomic force microscope, as shown in Figure 4(a, b, and c). The figures showed the smooth morphology of the zirconia layer at 0 g/L (Figure 2.a); however, the morphology was less smooth for Ni-P upon the addition of 10 and 20 g/L of nano-ZrO_2 (Figures 2 b &c).

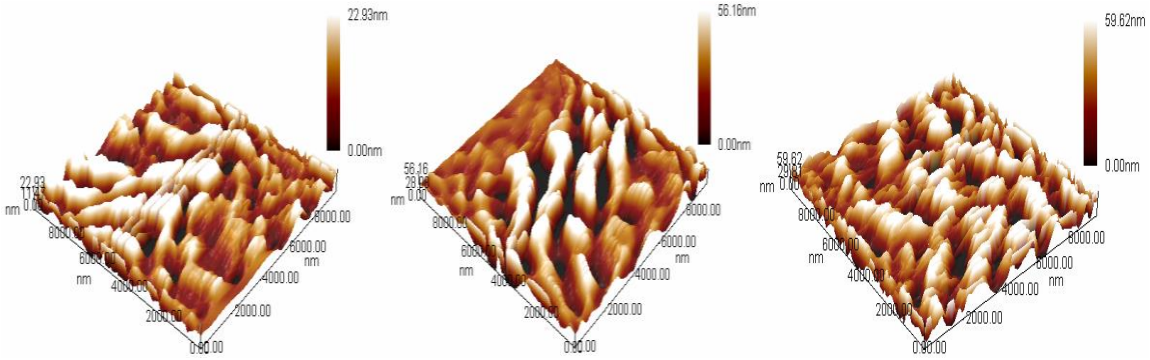

(a) **(b)** **(c)**

(a): Ni-P (b): Ni-P-10ZrO_2, (c): Ni-P-20ZrO_2

Figure (4): AFM Pattern of a specimen at (a), (b) and (c)

3.4 Hardness results

The effect of Ni-P, Ni-P-10ZrO_2 and Ni-P-20ZrO_2 coatings on the hardness value of the base metal was determined using the hardness test. The test also aimed to determine the effect of different ZrO_2 contents and different nickel contents on the hardness values of the base metal and the coatings. The results of the hardness test for the base metal and the coatings was presented in Table 4. The observed hardness value between the coatings differed due to the different zirconia contents in the layers. The particle size exerted a significant effect on the material hardness as can be mathematically explained using the Hall-Petch relationship (Ahmed, 2011):

$$HV = H_O + K/\sqrt{d} \qquad \ldots(2)$$

whereas :

H_V: Hardness of material with small granular size.

Ho: Hardness material is multi-size granular (polycrystalline grain size).

K: Constant, represents the slope of the Hv hardness when drawing against, and it depends on the type of material.

$1/\sqrt{d}$: The diameter of the particle.

The Hall-Petch relationship is a theory that explains the reason for the high hardness values (520 Hv) of ultra-fine microstructures compared to the coarser particles of the same hardened material.

Table (4) the hardness value coated layers.

Layer coating	hardness value
St.st 316L	**260**
Ni-P	**410**
Ni-P-10ZrO_2	**490**
Ni-P-20ZrO_2	**520**

Wear Tests

The weight loss of each sample was converted to the respective density and the outcome of this test under the same conditions earlier mentioned are presented in Figures 5 (a, b, c and d) previously (F: 10 N); ω: 300 rpm; (t: 5, 10, 15, and 20) min.

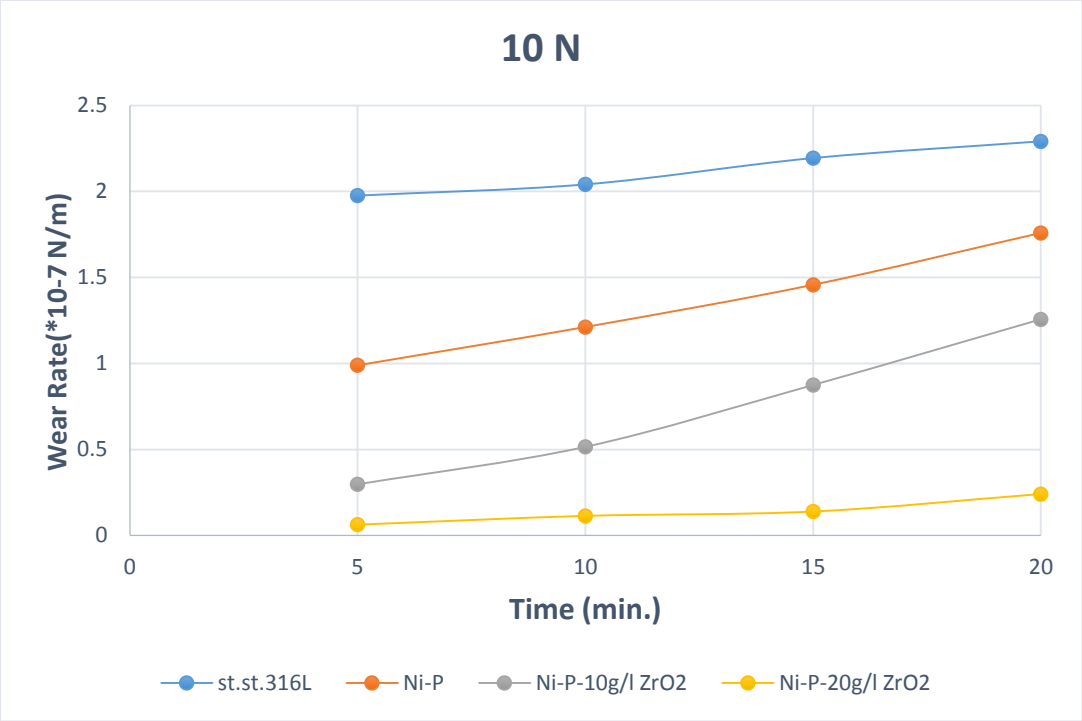

Figure (5) Wear rate of samples at (10 N) loads.

All through this study, the optimum thickness (37.9µm) was found to be more than the deposited layer thickness. A layer thickness of <20 µm is considered non-protective.

Figure 5 showed that the wear rate continued to increase with load values at a constant velocity due to an increasing rate of sub-surface deformation. This was supported by the results of (Srivastava et al., 2008), which found that wear rate increases linearly at a higher sliding distance. The study found that Ni coatings exhibited the most improved properties (in terms of better strength, higher wear, better adhesion, and better corrosion resistance) when compared with the properties of the conventional coarse-crystalline coatings.

The results also showed an increase in the volume loss with time due to the increase in particles loss at prolonged friction time. The effect of adding zirconia particles to the electroless-deposition solution on the wear rates was also studied at different conditions. The results showed a significant reduction in volume loss as the zirconia content increases, reaching the minimum value at the zirconia amount of 20 g/L as a result of the role of ZrO2 in increasing the hardness of the coated layers, thereby increasing the wear resistance. The reason for the thick layers could be due to the defects and loss of adhesion observed in the coated layer with 10 g/L ZrO2 after 15 min.

Conclusion:

1. All the coatings showed that the Ni-P & Ni-P-ZrO2 composite coatings are completely covered by microparticles of about 30-70 µm average grain size.
2. Ni-P-ZrO_2 composite layer showed a stable structure with a good level of crystallization and surface mechanical bonding as a result of the good interaction between ZrO_2 and the Ni-P matrix.
3. The base metal exhibited the highest wear rate at 40N while the wear rate decreased in the Ni-Pb-ZrO_2-coated SS316L by 34 %.
4. The Vickers hardness values of the Ni-P-ZrO_2 coated samples at different ZrO_2 contents (0, 10 and 20 g/L) were 19, 50, and 81%, respectively.

References:

1. Agarwala, R. C., & Agarwala, V. (2003). Electroless alloy/composite coatings: A review. *Sadhana*, *28*(3–4), 475–493.
2. Ahmed, J. K. (2011). Improvement the hardness and wear of (Zn-Ni) coating layer by adding silicon carbide. *Iraqi Journal of Mechanical and Material Engineering*, *11*(3).
3. Al-khafaji, Z. S., Radhi, N. S., & Mohson, S. A. (2018). Preparation and modelling of composite materials (polyester-alumina) as implant in human body. *International Journal of Mechanical Engineering and Technology*, *9*(4).
4. Al-Mimar, H. S., Awadh, S. M., Al-Yaseri, A. A., & Yaseen, Z. M. (2018). Sedimentary units-layering system and depositional model of the carbonate Mishrif reservoir in Rumaila oilfield, Southern Iraq. *Modeling Earth Systems and Environment*, *4*(4), 1449–1465. https://doi.org/10.1007/s40808-018-0510-5
5. Al-Zubaidy, B., Radhi, N. S., & Al-Khafaji, Z. S. (2019). Study the effect of thermal impact on the modelling of (titanium-titania) functionally graded materials by using finite element analysis. *International Journal of Mechanical Engineering and Technology*, *1*.
6. Apachitei, I., Duszczyk, J., Katgerman, L., & OVERKAMP, P. J. B. (1998). Electroless Ni-P composite coatings: the effect of heat treatment on the microhardness of substrate and coating. *Scripta Materialia*, *38*(9), 1347–1353.
7. Ashtiani, A. A., Faraji, S., Iranagh, S. A., & Faraji, A. H. (2017). The study of electroless Ni–P alloys with different complexing agents on Ck45 steel substrate. *Arabian Journal of Chemistry*, *10*, S1541–S1545.
8. Balaraju, J. N., Narayanan, T. S. N. S., & Seshadri, S. K. (2003). Electroless Ni–P composite coatings. *Journal of Applied Electrochemistry*, *33*(9), 807–816.
9. Brenner, A, & Riddell, G. E. (1946). Electroless plating by a process of controlled self continuing reduction. *Proc Amer Eletropl Soc*, *33*, 16.
10. Brenner, Abner. (1946). Nickel plating on steel by chemical reduction. *J. Res. NBS*, *37*, 31–34.
11. Dawood, N. M., Radhi, N. S., & Al-khafaji, Z. S. (2020). *Investigation Corrosion and Wear Behavior of Nickel-Nano Silicon Carbide on Stainless Steel 316L*. *1002*, 33–43.
12. Domenech, S. C., Lima Jr, E., Drago, V., De Lima, J. C., Borges Jr, N. G., Avila, A. O. V, & Soldi, V. (2003). Electroless plating of nickel–phosphorous on surface-modified poly (ethylene terephthalate) films. *Applied Surface Science*, *220*(1–4), 238–250.
13. Grosjean, A., Rezrazi, M., & Bercot, P. (2000). Some morphological characteristics of the incorporation of silicon carbide (SiC) particles into electroless nickel deposits. *Surface and Coatings Technology*, *130*(2–3), 252–256.
14. Grosjean, A., Rezrazi, M., Takadoum, J., & Bercot, P. (2001). Hardness, friction and wear characteristics of nickel-SiC electroless composite deposits. *Surface and Coatings Technology*, *137*(1), 92–96.
15. Guglielmi, N. (1972). Kinetics of the deposition of inert particles from electrolytic baths. *Journal of the Electrochemical Society*, *119*(8), 1009.
16. Kadhim, K. N., & Al-Rufaye, A. H. R. (2016). The Effects of Uniform Transverse Magnetic Field on Local Flow and Velocity Profile. *International Journal of Civil Engineering and Technology (IJCIET)*, *7*(2).
17. Li, Y. (1997). Investigation of electroless Ni-P-SiC composite coatings. *Plating and Surface*

Finishing, *84*(11), 77–81.

18. Mallory, G. O., & Hajdu, J. B. (1990). *Electroless plating: fundamentals and applications*. Cambridge University Press.
19. Nabaa S. Radhi et al. Nabaa S. Radhi et al.,. (2018). Investigation Biomedical Corrosion of Implant Alloys in Physiological Environment. *International Journal of Mechanical and Production Engineering Research and Development*, *8*(4), 247–256. https://doi.org/10.24247/ijmperdaug201827
20. none. (2009). Transactions of the Institute of Metal Finishing 2009, Volume 87. *Transactions of the IMF*, *87*(6), 330–332.
21. Radhi, N.S., & Al-Khafaji, Z. (2018). Investigation biomedical corrosion of implant alloys in physiological environment. *International Journal of Mechanical and Production Engineering Research and Development*, *8*(4). https://doi.org/10.24247/ijmperdaug201827
22. Radhi, Nabaa S. (2015). *Preparation, Characterization, and Modeling Functionally Graded Materials in Bio-application*. PhD thesis. University of Technology. Iraq.
23. Sahoo, P., & Das, S. K. (2011). Tribology of electroless nickel coatings–a review. *Materials & Design*, *32*(4), 1760–1775.
24. Sarret, M., Müller, C., & Amell, A. (2006). Electroless NiP micro-and nano-composite coatings. *Surface and Coatings Technology*, *201*(1–2), 389–395.
25. Srivastava, M., Grips, V. K. W., & Rajam, K. S. (2008). Influence of SiC, Si3N4 and Al2O3 particles on the structure and properties of electrodeposited Ni. *Materials Letters*, *62*(20), 3487–3489.
26. Xiang, Y., Zhang, J., & Jin, C. (2001). Study of Electroless NI-P Nan-meter Diamond Composite Coatings. *Plating and Surface Finishing*, *88*(2), 64–67.
27. Yaseen, Z. M., Aldlemy, M. S., & Oukati Sadegh, M. (2019). Non-gradient probabilistic Gaussian global-best harmony search optimization for first-order reliability method. *Engineering with Computers*. https://doi.org/10.1007/s00366-019-00756-7